Impact-Echo Nondestructive Testing and Evaluation with Hilbert-Huang Transform

Ruichong Zhang and Abdennour C. Seibi

***Abstract*—** This study proposes the implementation of Hilbert-Huang transform (HHT) time-frequency analysis in impact-echo (IE) testing for improved accuracy in integrity appraisal and damage diagnosis of infrastructure systems. In particular, this paper first reviews the fundamental of IE non-destructive testing and evaluation, i.e., formula of thickness estimation which is based on one-dimensional wave propagation and dependent upon the selected longitudinal wave speed of the materials under test, resonance frequency identified with fast Fourier transform (FFT) of IE recordings, and a shape-based correction factor. While this study details multiple causes of the distorted thickness estimation with the formula from the mechanics point of view, FFT-based analysis is among the most important factors. A time-frequency HHT analysis is then introduced to overcome the shortage of FFT analysis in identifying the resonant frequency from noise-added IE recordings. With FFT and HHT analyses of five data sets of sample IE recordings from sound and damaged concrete structures and comparison with referenced ones, this study reveals that the proposed IE approach with HHT analysis not only eliminates the subjective use of correction factor in the formula, it also improves greatly the accuracy in the thickness estimation.

***Keywords*—** Impact-Echo, Wave Propagation, Non-Destructive Testing and Evaluation, Hilbert-Huang Transform.

I. Introduction

Impact-echo (IE) approach of non-destructive testing (NDT) is widely used for non-destructive evaluation (NDE) of integrity and damage of various concrete and steel structures, exemplified as building beams/columns/walls, bridge decks, tunnel walls, post-tensioned ducts, pavements, and pipes. As schematically shown in Fig. 1, elastic impact of a steel sphere (denoted as impactor in the figure) on a tested or working surface of a structure generates longitudinal waves, which travel back and forth between the working surface and other side of the structure or the internal face of defects like crack, honeycomb, delamination or void. Analysis of the wave echo signals received at the transducer position next to the impact location in general, and finding the resonant frequency with fast Fourier transform (FFT) data analysis in particular, helps determine the depth of the structure or depth to the internal defect, which can help evaluate the structural integrity and diagnose internal damage. Some IE equipments, exemplified as simple Concrete Thickness Gauge (CTG) and comprehensive NDE360 of Olson Instruments, Inc., are shown in Figs. 2 and 3.

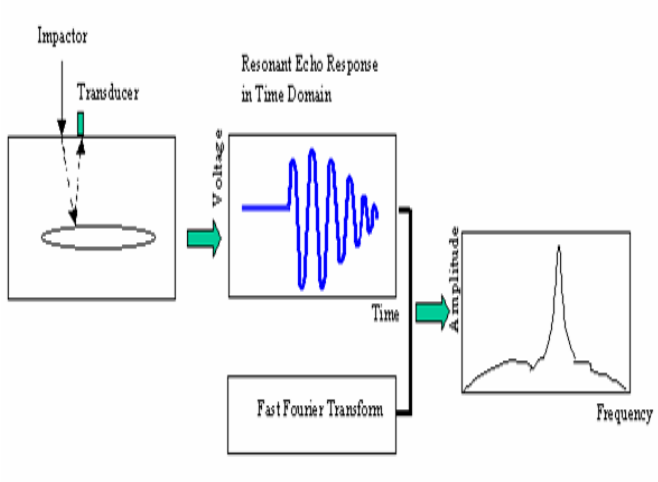

Fig. 1 Schematic of impact-echo approach in non-destructive testing and evaluation (Courtesy of L.D. Olson).

Fig. 2 Top view of IE equipments of Olson Engineering, Inc., in which the left is the IE scanner used for NDE360 and the right the traditional IE unit used for CTG (Courtesy of L.D. Olson).

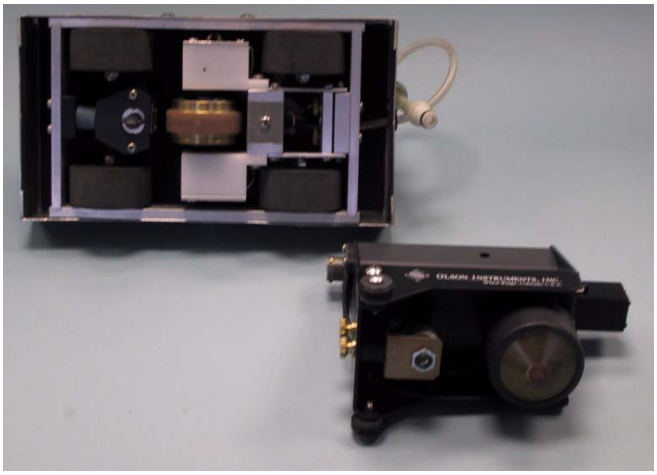

Fig. 3 Bottom view of IE equipments of Olson Engineering, Inc., in which the IE scanner in the top left has automatic impactor located in the middle left of the scanner bottom and rolling displacement transducers in the middle of the scanner, and the traditional IE unit for CTG in the bottom right has the impactor and transducer located in the left- and right-side positions of the CTG respectively (Courtesy of L.D. Olson).

The fundamental to the IE approach is based on one-dimensional wave propagation theory or formula for the thickness of the structure h or thickness to the internal defects [1]-[2]

$$h = \frac{\beta c}{f} \tag{1}$$

where f is resonant frequency identified with FFT data analysis of wave echo in IE recording, c the longitudinal or P-wave speed, and β the empirical correction factor accounting for the shape of the structure when it was first introduced, which takes 0.96 for plate structures [1] and ranges from 0.87 to 0.96 dependent upon the size of the structure [3], among others.

The less-than-unit correction factor in Eq. (1) implies that the thickness is typically overestimated with a given P-wave speed and resonant frequency measured from wave echo recording if no correction factor is considered or β=1. Recent studies [3]-[6] attribute the overestimation or correction factor to wave scattering and/or dispersion features resulted from two- or three-dimensional wave propagation in the structure with a finite size and different boundaries. While the aforementioned studies, together with many others, advance understanding of the role of correction factor in Eq. (1) and subsequently improve accuracy for thickness estimation, the perspective for correction factor is limited and suggested values to be used in the IE approach is subjective. This paper in the following sections tries to examine broadly the cause of the overestimation from the mechanics perspective and then propose an alternative way to eliminate the use of the subjective correction factor, while still improving accuracy of the IE approach for NDT/E.

II. Mechanics of Thickness Formula

Examining any kind of IE equipments exemplified in Figs. 2 and 3 suggests that the impact position (impactor in Fig. 1) has a non-negligible distance away from the wave-signal receiver (transducer in Fig. 1) on the working surface in comparison with the thickness to be estimated. This indicates that the echoed P-waves received are not travelling back and forth along the thickness h, but a slightly larger $h'=h/\beta_h$ with correction factor for thickness $\beta_h<1$. In other word, h in Eq. (1) should be replaced with h'. For simplicity in examining all the parameters used in Eq. (1), the empirical correction factor β is not considered, which will be elaborated later. Eq. (1) then becomes

$$h = \frac{\beta_h c}{f} \tag{2}$$

Because of the impact-to-receiver surface distance, the problem at hand should be tackled at least within the framework of two-dimensional, in-plane wave propagation in which both P-waves and shear or S-waves are coupled at free, fixed, and/or continuity boundaries, showing wave scattering phenomena in reflection and refraction or reflected and transmitted P- and S-waves from incident P-waves (or S-waves). This yields the echoed waves at the receiver not solely from traveling P-waves, but also from traveling S-waves. Considering the non-perfectly-vertical direction of the impactor and/or transducer to the working surface, one can expect the echoed wave signals at the receiver contain non-negligible S-wave signals in comparison with the P-waves. The mixed P- and S-wave echo will alter the period or frequency of pure P-wave echo shown in the recording, although the effect might be minor. With the fact that S-wave speed is smaller than the P-wave one, all the above suggests that use of P-wave speed in Eq. (1) or (2) provides the upper-bound solution for the thickness estimation. At this junction, a realistic smaller wave speed should be used in Eq. (1), i.e., $c'=\beta_c c$ with correction factor for wave speed $\beta_c<1$, or Eq. (2) is modified as

$$h = \frac{\beta_h \beta_c c}{f} \tag{3}$$

It is of interest to note that surface waves and wave scattering due to structural size and boundaries should not play a major role in the correction factor, while the influence of wave dispersion features needs further quantitative study, which is elaborated below. First, the impact-to-receiver surface distance is so small such that surface waves like non-dispersive Rayleigh (along a free surface) and Stoneley (along a two-layer boundary) waves are not well developed. Second, the geometrical and material damping makes the intensity of wave signals reflected from the boundaries in the non-thickness directions much weaker than that of waves echoed from the thickness direction, for the distance of the receiver to the former boundaries is typically much longer than that to the latter. Third, dispersive wave features may influence the correction factor only when Eq. (1) is used for estimating the thickness to the internal defect, which is strongly dependent upon type/size and direction of the defect relative to the

structural thickness and surface horizontal direction respectively.

With the use of FFT data analysis for displacement response recording at IE receiver, the resonance frequency in Eq. (1) or (3) is typically identified as the dominant frequency with local-maximum Fourier amplitude in Fourier amplitude spectrum of the recording. Fourier amplitude at a given frequency is associated with harmonic component defined globally over the entire time duration of the recording under investigation and thus meaningful only for stationary data analysis. For the recording at hand which is apparently nonstationary due to different arrivals of *P*- and *S*-waves and surface waves, and wave scattering and dispersion, the dominant frequency obtained with FFT essentially gives average, not true, characteristic of resonant frequency over the entire duration of the recording. While the use of short-time or windowed Fourier transform may possibly minimize the nonstationarity in the data caused by different types of wave echo, it cannot resolve the issues of nonstationarity rooted in the wave dispersion. In addition, windowed FFT, or selection of window length for FFT in particular, is subjective. To this end, a modified resonant frequency should be used in Eq. (3), i.e., $f=f'/\beta_f$ with β_f denoting correction factor for resonant frequency that is compensated for FFT-based average frequency identification (f'). To this end, Eq. (3) can be corrected as

$$h = \frac{\beta_h \beta_c \beta_f c}{f} = \frac{\beta c}{f} \tag{4}$$

With the aforementioned understanding, correction factor β used in Eq. (1) can be regarded as one combining those three, i.e., $\beta = \beta_h \beta_c \beta_f$.

In principle, thickness can be estimated with improved accuracy if the correction factor is given. In practice, it is almost impossible for having the correction factor corresponding to different shape, size, and boundaries of structure and defects under NDT/E. Nevertheless, recognizing that the influence of correction factors for thickness and wave speed has been implicitly shown in the resonant frequency of the recording, and the resonant frequency changes slightly from time to time in the entire duration of nonstationary recording, one can use time-frequency data analysis for identifying the true resonant frequency and thus abandon the use of correction factor, which is detailed below.

III. Hilbert-Huanng Transform

Alternative to the FFT data analysis and other means [7]-[10], this study proposes the use of HHT time-frequency data analysis for nonstationary recording [11]-[12] to depict nonstationary features in general, and identifying resonance frequency in particular, from IE recordings.

The HHT method consists of empirical mode decomposition (EMD) and Hilbert spectral analysis (HSA). Any complicated time domain record can be decomposed via EMD into a finite, often small, number of intrinsic mode functions (IMF) that admit a well-behaved Hilbert transform. The IMF is defined by the following conditions: (1) over the entire time series, the number of extrema and the number of zero-crossings must be equal or differ at most by one, and (2) the mean value of the envelope defined by the local maxima and the envelope defined by the local minima is zero at any point. An IMF represents a simple oscillatory mode similar to a sinusoidal component in FFT analysis, but more general.

The EMD explores temporal variation in the characteristic time scale of the data and thus is adaptive to nonstationary data processes. It functions as a dyadic filter for broad-band noise data [13]. The HSA defines an instantaneous or time-dependent frequency of the data via Hilbert transformation of each IMF component.

The HHT representation of IE recording $X(t)$ is

$$X(t) = \Re \sum_{j=1}^{n} a_j(t) e^{i\theta_j(t)} = \Re \sum_{j=1}^{n} [C_j(t) + iY_j(t)] \tag{5}$$

where $\Re$ denotes taking the real part, $C_j(t)$ and $Y_j(t)$ are respectively the j-th IMF component of $X(t)$ and its Hilbert transform $Y_j(t) = \frac{1}{\pi} P \int \frac{C_j(t')}{t - t'} dt'$ with P denoting the Cauchy principal value, and the time-dependent amplitudes $a_j(t)$ and phases $\theta_j(t)$ are the polar-coordinate expression of Cartesian-coordinate expression of $C_j(t)$ and $Y_j(t)$, from which the instantaneous frequency is defined as $\omega_j(t) = d\theta_j(t)/dt$. The Hilbert amplitude spectrum $H(\omega, t)$ and marginal Hilbert amplitude spectrum $h(\omega)$ over time duration T of the data are defined as

$$H(\omega, t) = \sum_{j=1}^{n} a_j(t) \tag{6}$$

$$h(\omega) = \int_0^T H(\omega, t) dt \tag{7}$$

While the Hilbert and marginal Hilbert amplitude spectra provide information similar to the Fourier amplitude spectrum obtained from short-time Fourier transform, its frequency term is different. Fourier-based frequency is constant over the harmonic function persisting through the data window, while HHT-based frequency varies with time. As the Fourier transformation window length reduces to zero, the Fourier-based frequency approaches the HHT-based frequency. Fourier-based frequency is, however, locally averaged and not truly instantaneous for it depends on the window length. Because of the aforementioned unique HHT features, the dominant frequency identified from marginal Hilbert amplitude spectrum is expected closer to the true resonant frequency than that from Fourier amplitude spectrum.

The difference of FFT and HHT can be seen from analyzing a hypothetical record $y(t) = y_1(t) + y_2(t)$ in Fig. 4, where nonstationary wave signal $y_1(t) = \cos[2\pi t + \varepsilon \sin(2\pi t)] e^{-0.2t}$ has time-dependent frequency of $1+\varepsilon\cos(2\pi t)$ *Hz* bounded by $1-\varepsilon$ and $1+\varepsilon$ with ε denoting a small factor, and stationary noise without damping $y_2(t) = 0.05\sin(30\pi t)$ has constant or time-independent frequency of 15 *Hz*. Note that the waves

have a non-sinusoidal waveform with sharp crests and rounded-off troughs.

The wave signal can be expanded into and thus interpreted by a series of stationary waves, as is done in Fourier spectral analysis; for example, $y(t)$ can be understood as to contain Fourier components at all frequencies, as shown in Fig. 5.

Alternatively, Taylor expansion of $y_1(t) \approx [-0.5\varepsilon + \cos(2\pi t) + 0.5\varepsilon\cos(4\pi t)]e^{-0.2t}$, *for* $\varepsilon << 1$ suggests that Fourier transform of $y_1(t)$ consists primarily of two harmonic functions at respectively 1 and 2 *Hz*, and the width of these two harmonic functions in Fourier amplitude spectrum in Fig. 5 is proportional to the exponential parameter 0.2 that is related to damping factor. Note that Figs. 4 and 5 use ε=0.5 that is not a small number in comparison with unit. Therefore, the Fourier amplitude spectrum in Fig. 5 shows the third observable peak at 3 *Hz*. One can equally well describe $y_1(t)$ by saying that it consists of just two frequency components for $\varepsilon<<1$, each component having a time varying amplitude that is proportional to $e^{-0.2t}$.

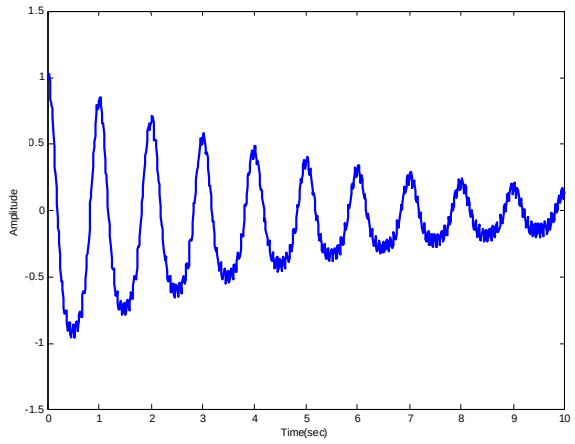

Fig. 4 A hypothetical wave recording, consisting of wave signal and noise with frequencies being 1+0.5cos(2πt) and 15 in Hz, respectively.

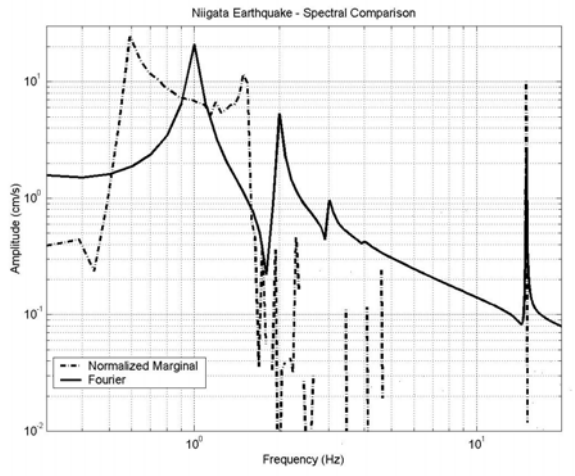

Fig. 5 Fourier and marginal Hilbert amplitude spectra of the recording in Fig. 4.

Because the true frequency content of the wave signal $y_1(t)$ is bounded between 1-ε and 1+ε, much less than 2 *Hz*, analysis of the record suggests that FFT typically distorts the nonstationary data. Similar assertions are concluded in [11]-[12], among others, with the aid of solutions to classic nonlinear systems. On the other hand, HHT-based mar

By contrast, the marginal Hilbert amplitude spectrum in Fig. 5 shows truthfully the amplitude distribution of the motion in frequency bounded by 0.5 and 1.5 *Hz* for nonstationary waves and 15 *Hz* for noise.

While the broad-based applications of the HHT in time-frequency data analysis in general, and some advantages over FFT in particular, can be found in [14]-[15] and [16]-[21] respectively, among many others, most data analyzed are broad-band. In other words, HHT analysis of narrow-band data such as IE recordings is rarely seen. This is likely due to the drawback of EMD for narrow-band data process, i.e., lack of some frequency-band contents or equivalently characteristic time scales in recordings may sometimes make the EMD to mix two widely-separate scale signals into one IMF or separate similar scale signals to different IMFs, resulting in aliasing in time-frequency distribution. To solve the mode mixing issue and enable the EMD work for narrowband data in all the cases, a simple, yet proved to be sound and effective, way is to add a finite-amplitude, white noise into the original data in [13] and [22]. The noise-added data is by nature broad-band without change of the frequency distribution, which prepares the HHT analysis effectively for revealing quantifies like resonant frequency from marginal Hilbert amplitude spectrum.

IV. Validation with IE Recordings

To illustrate the proposed IE approach with modified data analysis, this study examines five sets of IE recordings for sound and damaged concrete plate structures, provided by Olson Engineering, Inc. The *P*-wave speed for all the five samples is 30,480 *m/s*, and the thicknesses of the sample structures are listed in Table 1, in which samples 3 and 4 have internal defects corresponding to the shorter thicknesses. These thicknesses could be estimated based on Eq. (1) as well as Fourier-based data analyses such as high-pass filter, smoothing windows and resonant frequency identification. Since the thicknesses of sample structures can be easily validated with direct measurements, all the data listed in Table 1 may reasonably be regarded as referenced, correct thicknesses.

For comparison of IE approach with FFT and HHT data analyses, Eq. (1) without correction factor and unprocessed, raw recordings are used. Figures 6 and 7 show respectively the raw recordings of samples 1 and 3, which contains significant energy in the very low frequency band, resulting from pushing down the IE equipment like CTG in testing for better contact between IE equipment and working surface, dominant wave echo signals in the narrow frequency band, as well as few others like noise in high-frequency band which are not easily observed from the time history.

Table 1 Referenced thicknesses of five sample concrete structures, in which the smaller number in samples 3 and 4 corresponds to the thickness to the internal defect.

Sample No.	Referenced Thickness in *cm*	
1	26.92	
2	26.42	
3	41.15	15.49
4	25.65	21.59
5	27.43	

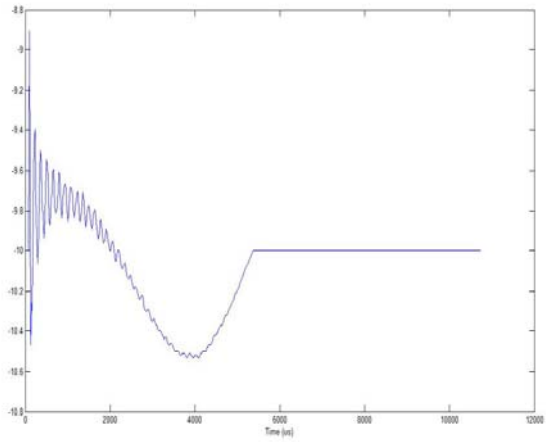

Fig. 6 Unprocessed, raw displacement time-history recording for sample 1.

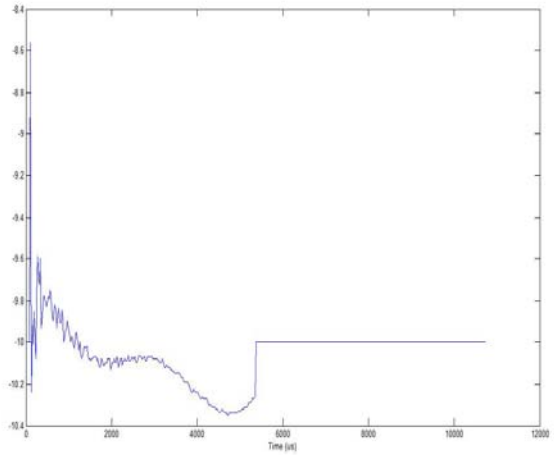

Fig. 7 Unprocessed, raw displacement time-history recording for sample 3.

With the FFT analysis of recordings in Figs. 6 and 7, Fourier amplitude spectra of samples 1 and 3 are shown in Figs. 8 and 9 respectively, from which the marked dominant frequencies can be identified, which are shown in Table 2. With those identified resonance frequencies and the use of Eq. (1) without correction factor, the pertinent thicknesses can be found in Tables 3, in which relative errors with referenced thicknesses are also calculated.

Table 2 Identified resoance frequencies with FFT data analysis of unprocessed, raw IE recordings

Sample No.	FFT-based resonance frequencies in *Hz*				
1	7068				
2	7254				
3	4650	5487	11900	12090	12280
4	7347	7533	7719	8836	
5	6882				

Table 3 Estimated thicknesses and calculated relative errors with FFT analysis

Sample No.	FFT-based Thickness in *cm* (Relative Error in %)				
1	27.61 (2.5)				
2	26.90 (1.8)				
3	41.91 (1.8)	35.56 (13.6)	16.51 (5.8)	16.26 (4.1)	16.00 (2.5)
4	26.67 (4.0)	25.91 (1.0)	25.15 (1.5)	22.10 (2.3)	
5	28.35 (3.3)				

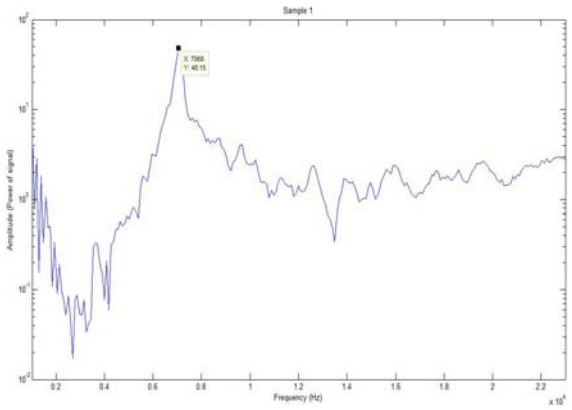

Fig. 8 Frequency amplitude spectrum of displacement response for sample 1, in which marks at some peaks are related to the resonant frequencies used in Eq. (1), and amplitude is in logarithmic scale and frequency in linear one.

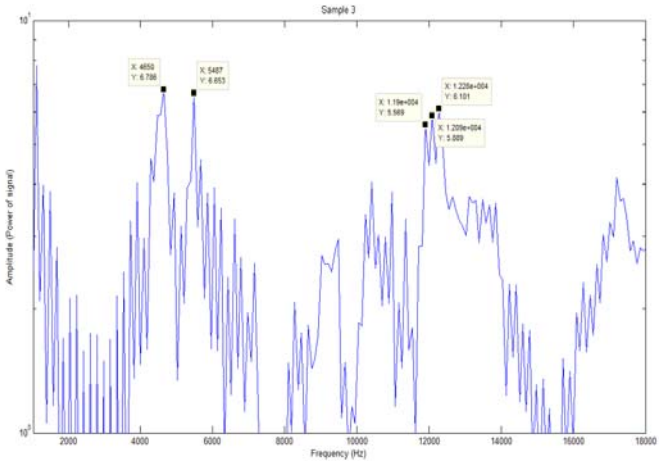

Fig. 9 Frequency amplitude spectrum of displacement response for sample 3.

To facilitate the HHT analysis, a white noise is added into the raw recording, in which the white noise power is selected as 10% of original raw one. Figures 10 and 11 show respectively the marginal Hilbert amplitude spectra of samples 1 and 3, from which the marked dominant frequencies are shown in Table 4. With the use of Eq. (1) without correction factor, the pertinent thicknesses can be found in Table 5, in which relative errors with referenced thicknesses are also calculated.

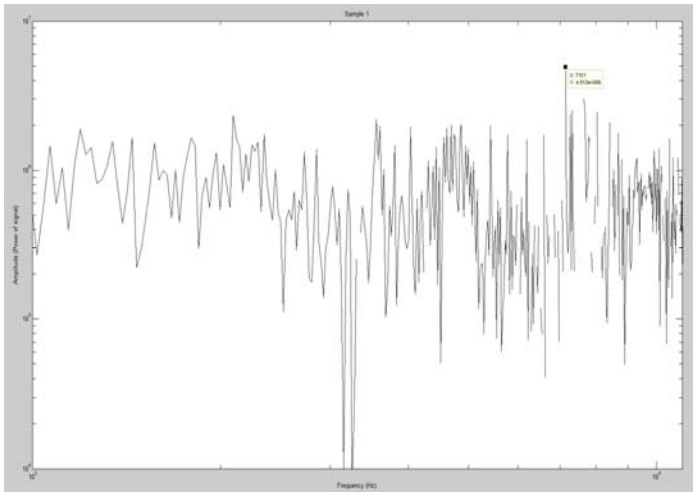

Fig. 10 Marginal Hilbert amplitude spectrum of noise-added displacement response for sample 1, in which marks at some peaks are related to the resonant frequencies used in Eq. (1), and both amplitude and frequency are in logarithmic scale.

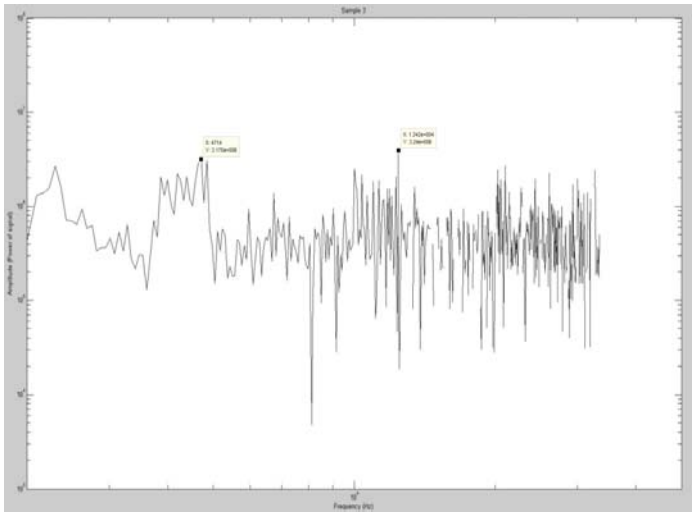

Fig. 11 Marginal Hilbert amplitude spectrum of noise-added displacement response for sample 3.

Comparison of Tables 3 and 5 indicates clearly the improved accuracy with HHT analysis over the traditional FFT analysis, which can be elaborated below. First, the relative errors for estimating all the thicknesses are significantly reduced with the HHT analysis from those with traditional FFT analysis, indicating the significant improvement of accuracy for thickness estimation. Second, the HHT analysis can identify uniquely defect-related resonant frequencies and subsequently the pertinent thicknesses, while the FFT sometimes provides multiple peaks in Fourier spectrum as shown in Fig. 9, resulting in multiple resonant frequencies and thicknesses. Third and most important, the thickness estimation with FFT is higher than the referenced one in each and every sample, suggesting that the dominant frequency identified with FFT (f) should be smaller than the resonant frequency (f') used in Eq. (1), or $f'= f/\beta$ with $\beta<1$. In other words, correction factor β can be explained as compensation for the inaccurate FFT-based identification of resonant frequency, alternative to the correction for structural shape as introduced in Eq. (1) in the early stage. Note again that the influence of correction factors for thickness and wave speed are not taken into account, for that is inherited in the recording under investigation, or equivalently the resonant frequency identified from the recording should genetically account for the influence of those two factors. Since the HHT analysis can explore the resonant frequency more truthfully than the FFT one, the correction factor is not necessarily used for estimating thickness with Eq. (1).

Table 4 Identified resoance frequencies with HHT data analysis of noise-added IE recordings

Sample No.	HHT-based resonance frequencies in *Hz*	
1	7151	
2	7363	
3	4714	12420
4	7563	8815
5	6979	

Table 5: Estimated thicknesses and calculated relative errors with HHT analysis

Sample No.	HHT-based Thickness in *cm* (Relative Error in %)	
1	27.25 (1.23)	
2	26.49 (0.29)	
3	41.38 (0.56)	15.70 (1.31)
4	25.78 (0.50)	24.33 (0.14)
5	27.94 (1.85)	

V. Conclusion

This study examines rationale of the thickness estimation formula, which is based on one-dimensional, longitudinal wave propagation theory and widely used for evaluating integrity and damage of structures with an IE approach. The investigation addresses the multiple influences of the two-dimensional wave propagation and resonant frequency

identification in the formula in general and correction factor in particular. It is found that the correction factor used in the formula should not be designated for influence of the structural shape, as originally proposed. Instead, it combines influences of measurement of dominant frequency for data analysis, dominant wave propagation path, wave scattering and dispersion due to the boundary conditions in structure and defects. After indicating the limitation of traditional FFT data analysis in identifying resonant frequency, this study proposed the use of time-frequency HHT analysis of noise-added recordings. Numerical examples of five sets of raw IE recordings from sound and damaged structures show not only the significantly-improved accuracy in thickness estimation with proposed IE approach, but also demonstrate that the correction factor can be dropped out from the thickness formula.

It should be pointed out that the results from this study are based on qualitative analysis of thickness formula from mechanics viewpoint and verified with a limited number of IE recordings. They must, therefore, be validated further by model-based simulation (e.g., [23]-[25]) and recordings-supply analysis, which will be reported later.

While the proposed HHT analysis of noise-added recordings does improve the thickness estimation accuracy, other alternative approaches may equivalently do the same or further advances it. One is the use of Hilbert transform analysis of recordings instead of HHT, if the recordings admit a well-behaved Hilbert transform, i.e., no non-physical instantaneous frequency was withdrawn from the Hilbert transform. Readers are referred to [11]-[12] for detail. The other is to perform the statistical analysis of IMFs of EMD for noise-added recordings, for the realizations of each and every white noise will be cancelled out in calculating the ensemble average of IMFs, leaving the true IMFs pertinent to the original recording. The theory and advantage of this statistical data process, termed as ensemble EMD or EEMD can be found in [22]. The aforementioned two are subjective to further studies.

ACKNOWLEDGMENT

The authors would like to express their sincere gratitude to P. Miller of Olson Engineering, Inc. for supplying IE recordings, L.D. Olson, President and Principal Engineer of Olson Engineering, Inc. for providing some figures and constructive suggestions, and A. Helal, A. Khalil, and M. Rahim from Petroleum Institute in United Arab Emirates for providing computation in section IV. This work was partially conducted when the first author took sabbatical leave from Colorado School of Mines (CSM) and guided senior design projects I and II in mechanical engineering program in Petroleum Institute (PI), Abu Dhabi, United Arab Emirates in 2009-2010. This work was supported by CSM–PI joint research project under the auspices of Abu Dhabi National Oil Company. The opinions, findings and conclusions expressed herein are those of the authors and do not necessarily reflect the views of the sponsors.

REFERENCES

[1] M. Sansalone and W. Streett, *Impact-Echo Nondestructive Evaluation of Concrete and Masonry*, Ithaca, NY: Bullbrier Press, 1997.

[2] ASTM C 1383, Test method for measuring the P-wave speed and the thickness of concrete plates using the impact-echo method, *2000 Annual book of ASTM Standards*, Vol. 04-02, ASTM, West Conshohocken, PA.

[3] D. Alver, M. Ohtsu, and H. Wiggenhauser, "Dynamic boundary element method analysis for correction factor determination in impact-echo," *Journal of Transportation Research Board*, Vol. 2050, 2008, pp. 122-126.

[4] N. Ryden and C.B. Park, "A combined multichannel impact echo and surface wave analysis scheme for non-destructive thickness and stiffness evaluation of concrete slabs." *AS NT, 2006 NDE Conference on Civil Engineering*, St. Louis, MO, 2006.

[5] C.L. Barnes and J.F. Trottier, "Hybrid analysis of surface wavefield data from Portland cement and asphalt concrete plates," *NDT&E International*, 42, 2009, 106-112.

[6] D. Alggernon, "Impact-echo data analysis based on duration and bandwidth of the signal components," *Journal of Transportation Research Board*, 2050, 2008, pp. 127-133.

[7] A. Toma, "The Fourier Transform of some distributions from D0(R) and D0(R2) with applications in mechanics" *Recent Advances in Acoustics $ Music,* Proceedings of the 11th WSEAS International Conference on Acoustics & Music: Theory & Applications (AMTA '10), "G. Enescu" University, Iasi, Romania, June 13-15, 2010. ISBN: 978-960-474-192-2 / ISSN: 1790-5095, pp 51-54.

[8] C. Guarnaccia, "Acoustical Noise Analysis in Road Intersections: a Case Study" *Advances in Acoustics $ Music,* Proceedings of the 11th WSEAS International Conference on Acoustics & Music: Theory & Applications (AMTA '10), "G. Enescu" University, Iasi, Romania, June 13-15, 2010. ISBN: 978-960-474-192-2 / ISSN: 1790-5095, pp 208-215.

[9] V.N. Ivanovic and S. Jovanovski, "Signal Adaptive Method for Improved Space/Spatial-Frequency Representation of Nonstationary Two-Dimensional Signals" *New Aspects of Signal Processing,* Proceedings of the 9th WSEAS International Conference on Signal Processing (SIP '10), Catania, Italy, May 29-31, 2010. ISBN: 978-954-92600-4-5 / ISSN: 1790-5117, pp 72-76.

[10] S. Abdullahi, T.E. Putra, M.Z. Nuawi, Z.M. Nopiah, A. Arifin and L. Abdullah, "Time-Frequency Localisation Analysis for Extracting Fatigue Damaging Events," *Recent Advances in Signal Proccessing, Robotics and Automation*, Proceedings of the 9th WSEAS International Conference on Signal Processing, Robotics and Automation (ISPRA '10), University of Cambridge, UK, February 20-22, 2010. ISBN: 978-960-474-157-1 / ISSN: 1790-5117, pp 31-35.

[11] N.E. Huang, S. Zheng, S.R. Long, M.C. Wu, H,H. Shih, Q. Zheng, N-C. Yen, C.C. Tung, and M.H. Liu. "The empirical mode decomposition and Hilbert spectrum for nonlinear and nonstationary time series analysis." *Proceedings of Royal Society of London, A* 454, 1998, 903-995.

[12] N.E. Huang, Z. Shen, and R.S. Long, "A new view of nonlinear water waves--Hilbert Spectrum," *Ann. Rev. Fluid Mech*. 31, 1999, 417-457.

[13] P. Flandrin, G. Rilling and P. Goncalves, "EMD equivalent filter banks, from interpretation to applications," H*ilbert-Huang Transform: Introduction and Applications*, eds. N.E Huang and S.S.P. Shen, World Scientific, Singapore, 2005, 67-87.

[14] N. Huang and Z. Wu, "A review on Hilbert-Huang transform: Method and its applications to geophysical studies," *Reviews of Geophysics*, 46, RG2006, 2008, 23 pages.

[15] N. Attoh-Okine, K. Barner, D. Bentil, and R. Zhang (Eds) "Special issue on The Empirical Mode Decomposition and the Hilbert-Huang Transform," *EURASIP Journal on Advances in Signal Processing*, 2008, 124 pages, 13 papers.

[16] R. Zhang, S. Ma, E. Safak, and S. Hartzell, "Hilbert-Huang transform analysis of dynamic and earthquake motion recordings," *ASCE Journal of Engineering Mechanics,* 129, 8, 2003, pp 861-875.

[17] R. Zhang, S. Ma, and S. Hartzell, "Signatures of the seismic source in EMD-based characterization of the 1994 Northridge, California, earthquake recordings," *Bulletin of the Seismological Society of America*, 93(1), 2003, 501-518.

[18] R. Zhang, R. King, L. D. Olson and Y.L. Xu, "Dynamic response of the Trinity River Relief bridge to controlled pile damage: modeling and

experimental data analysis comparing Fourier and Hilbert-Huang techniques," *Journal of Sound and Vibration*, 285, 2005, 1049-1070.
[19] R. Zhang, "Characterizing and quantifying earthquake-induced site nonlinearity," *Soil Dynamics and Earthquake Engineering*, 26, 2006, 799-812.
[20] R. Zhang, "A simple approach for quality evaluation of non-slender, cast-in-place piles," *Smart Structures & Systems*, 4, 2008, 1-15.
[21] R. Zhang, "A recording-based approach for identifying seismic site liquefaction and nonlinearity via HHT data analysis," *Advances in Adaptive Data Analysis*, 1, 2009, 89-123.
[22] Z. Wu and N. Huang, "Ensemble empirical mode decomposition: a noise-assisted data analysis method," *Advances in Adaptive Data Analysis*, 1, 2009, 1-41.
[23] R. Zhang, Y. Yong, and Y.K. Lin, "Earthquake ground motion modeling. I: Deterministic point source, and II: Stochastic line source" *Journal of Engineering Mechanics-ASCE*, 117(9), 1991, 2114-2132 and 2133-2150.
[24] R. Zhang, L. Zhang, and M. Shinozuka, "Seismic waves in a layered medium with laterally inhomogeneous layers. I: Theory, and II: Analysis" *Journal of Applied Mechanics-Transactions of The ASME*, 64(1), 1997, 50-58 and 59-65.
[25] R. Zhang, "Some observations on modeling of wave motion in a layer-based elastic medium," *Journal of Sound and Vibration,* 229(5), 2000, 1193-1212.

Ruichong Zhang received his B.S degree in engineering mechanics in 1984, M.S degree in structural engineering in 1987, both from Tongji University, Shanghai, China, and Ph.D. degree in mechanical engineering from Florida Atlantic University, Florida, USA in 1992. He is registered Professional Engineer in California, USA.

He holds Associate Professorship in Division of Engineering at Colorado School of Mines, Golden, Colorado, USA. Before joining Colorado School of Mines, Dr. Zhang had worked in Princeton University for three and a half years as Post-Doctoral Research Associate, and in University of Southern California for two years as Research Assistant Professor. He also took sabbatical leave from Colorado School of Mines and worked as Visiting Associate Professor in Department of Mechanical Engineering at Petroleum Institute, Abu Dhabi, United Arab Emirates in 2009-2010, in addition to his working as visiting scholar in Tongji University, Hong Kong Polytechnic University and Tianjing University in China in the summer of 2000, 2001 and 2003 respectively.

Dr. Zhang's research interest resides in continuum mechanics, vibration theory, wave propagation, stochastic processes and fields, and advanced data processing and analysis for sensory systems, disaster assessment and mitigation, and structural/geotechnical nondestructive evaluation and health monitoring. He is author of one edited book, one book chapter, one edited journal, thirty nine journal papers and numerous papers in conference proceedings and edited books. Dr. Zhang is the recipient of 1997 IASSAR Junior Research Prize in Stochastic Dynamics for his contribution to the solutions of seismic wave propagation through stochastic media, bestowed by International Association for Structural Safety and Reliability (IASSAR).

Abdennour C. Seibi received his B.S degree from the Mechanical Engineering in 1985 and M.S and PhD in Engineering Mechanics in 1988 and 1993 from the Pennsylvania State University. He is a distinguished researcher in problems related to the oil & gas sectors, has established international collaborations with various research labs and companies such as Shell Research Center, SEPTAR, in The Hague, the Institute of general Mechanics in Aachen, Germany, laboratoire de Mechanique in Rouen, France, and l'Ecole Polytechnique in Tunis. Has published extensively and his undergraduate students won seven international students papers awards from ASME/JSME, and managed to attract more than 3 million US Dollars research fund. His research area includes but not limited to the use of finite element analysis to solve engineering problems, tubular expansion, fatigue and fracture mechanics, and failure analysis of engineering materials. Recently, he is engaged on pipeline inspection project with Colorado School of Mines.